



Employing Temporal Properties of Brain Activity for Classifying Autism Using Machine Learning

Preetam Srikar Dammu^(✉) and Raju Surampudi Bapi

School of Computer and Information Sciences, University of Hyderabad,
Hyderabad, India

preetam.srikar@gmail.com, raju.bapi@iiit.ac.in

Abstract. Exploration of brain imaging data with machine learning methods has been beneficial in identifying and probing the impacts of neurological disorders. Psychopathological ailments that disrupt brain activity can be discerned with the help of resting-state functional magnetic resonance imaging (rs-fMRI). Research has revealed that brain connectivity is dynamic in nature and that its dynamic properties are affected by brain disorders. In the literature, numerous approaches have been proposed for identifying the presence of Autism Spectral Disorder (ASD), yet most of them do not consider brain dynamics in their diagnostic process. Significant amount of knowledge can be procured by taking the evolution of brain connectivity over time into account. In this work, we propose a new approach that leverages brain dynamics in the classification of autistic and neurotypical subjects using rs-fMRI data. We examined the proposed method on a large multi-site dataset known as ABIDE (Autism Brain Imaging Data Exchange) and have achieved state-of-the-art classification results with an accuracy of 73.6%. Our work has shown that taking the temporal properties of brain connectivity into account improves the classification performance.

Keywords: rs-fMRI · Autism detection · Dynamic FC

1 Introduction

Machine learning is being used extensively for identifying diseases of all kinds using biological data in the recent times. Neuroimaging of the brain produces high dimensional data which possesses abundant information regarding a person's mental health, emotions and cognitive activities. Disturbances in brain activity patterns caused by ailments which are imperceptible to humans owing to high dimensionality of the data can be recognized by machine learning methods.

Functional magnetic resonance imaging (fMRI) uses blood-oxygen-level dependent (BOLD) signals [10] to measure the level of activity of brain regions. It has been established by various studies that anomalies in cognitive functions

are induced by neurological diseases, and these aberrations are reflected in brain activity patterns [3, 12, 13, 15, 18, 24]. Hence, the information obtained from fMRI scans can be used to identify the presence of psychopathological disorders.

Functional Connectivity (FC) of the brain evolves over time and has multiple distinct states characterized by unique connectivity patterns [1, 4, 11].

Autism Spectrum Disorder (ASD) is a developmental disorder known to alter brain connectivity [3, 12, 13, 15, 24]. Taking brain dynamics into account has increased the accuracy in identifying subjects with ASD [22] which demonstrates that brain dynamics bear notable information about the disorder.

In this work, we leverage the temporal properties of brain connectivity to classify autistic and typically developing (TD) subjects from the ABIDE dataset [6]. We observed significant improvement in performance when compared to methods that do not consider brain dynamics.

2 Data Description

The Autism Brain Imaging Data Exchange (ABIDE) [6] is a collaborative project which consists of data from 17 different imaging sites. It is a diverse dataset comprising of data generated by different machines and scan parameters. The demographics of the participants varies highly from one site to another, as can be seen in Table 1. The heterogeneous nature of ABIDE dataset poses a challenge but also provides for better generalization [20].

2.1 Data Preprocessing

The Configurable Pipeline for the Analysis of Connectomes (CPAC) is a pipeline provided by Preprocessed Connectomes Project (PCP) which performs several preprocessing on the fMRI data. The Automated Anatomical Labeling (AAL) atlas has 116 region of interests (ROIs). Time series fMRI data used in this study uses the AAL parcellation and is preprocessed with the CPAC pipeline. Information regarding the steps involved in the CPAC pipeline is available on the ABIDE website (<http://preprocessed-connectomes-project.org/abide/>).

2.2 Participants

To sufficiently account for the temporal properties of brain connectivity, data from sites which have scan duration less than five minutes have not been considered. This step has resulted in the exclusion of four sites (Caltech, OHSU, Pitt & Trinity) leaving us with 14 different imaging sites and 869 participants (423 ASD, 446 TD). All of the subjects from the remaining sites included in a previous study which reported state-of-the-art accuracy have been included [8]. The demographics of the participants are presented in Table 1.

Table 1. Phenotypic details of the participants. [8] (†: Information unavailable, SD: Standard Deviation, FD: Mean Framewise Displacement, ADOS: Autism Diagnostic Observation Schedule [17])

Site	ASD			TD		FD
	Age mean (SD)	ADOS mean (SD)	Count	Age mean (SD)	Count	
CMU	26.4 (5.8)	13.1 (3.1)	M 11, F 3	26.8 (5.7)	M 10, F 3	0.29
KKI	10.0 (1.4)	12.5 (3.6)	M 16, F 4	10.0 (1.2)	M 20, F 8	0.17
LEUVEN	17.8 (5.0)	† (†)	M 26, F 3	18.2 (5.1)	M 29, F 5	0.09
MAX MUN	26.1 (14.9)	9.5 (3.6)	M 21, F 3	24.6 (8.8)	M 27, F 1	0.13
NYU	14.7 (7.1)	11.4 (4.1)	M 65, F 10	15.7 (6.2)	M 74, F 26	0.07
OLIN	16.5 (3.4)	14.1 (4.1)	M 16, F 3	16.7 (3.6)	M 13, F 2	0.18
SBL	35.0 (10.4)	9.2 (1.7)	M 15, F 0	33.7 (6.6)	M 15, F 0	0.16
SDSU	14.7 (1.8)	11.2 (4.3)	M 13, F 1	14.2 (1.9)	M 16, F 6	0.09
STANFORD	10.0 (1.6)	11.7 (3.3)	M 15, F 4	10.0 (1.6)	M 16, F 4	0.11
UCLA	13.0 (2.5)	10.9 (3.6)	M 48, F 6	13.0 (1.9)	M 38, F 6	0.19
UM	13.2 (2.4)	† (†)	M 57, F 9	14.8 (3.6)	M 56, F 18	0.14
USM	23.5 (8.3)	13.0 (3.1)	M 46, F 0	21.3 (8.4)	M 25, F 0	0.14
YALE	12.7 (3.0)	11.0 (†)	M 20, F 8	12.7 (2.8)	M 20, F 8	0.11

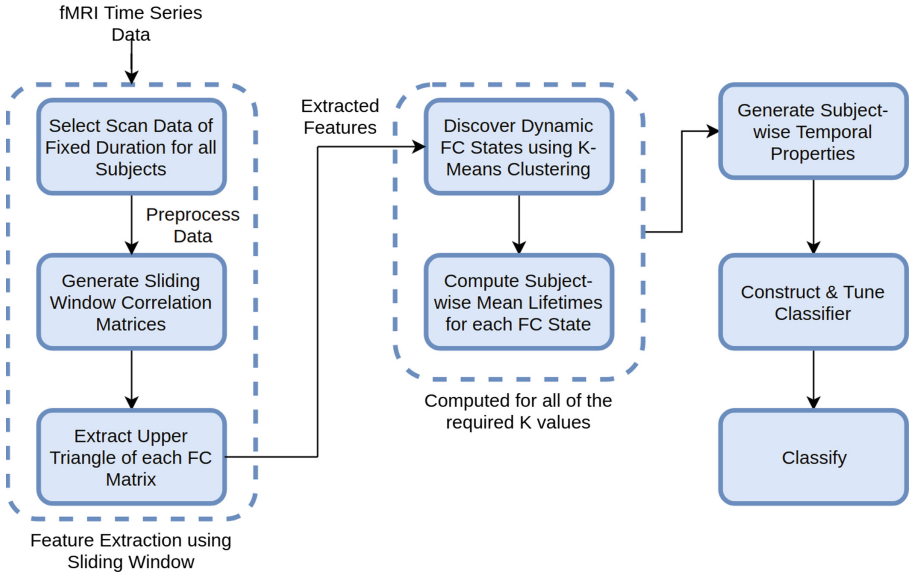


Fig. 1. Flowchart of the proposed Dynamic FC classification pipeline.

3 Methods

3.1 Proposed Dynamic FC Approach

In this work, we propose a new strategy to extract the temporal properties of brain connectivity and consequently use them as features to test for presence of autism.

When working with dynamic FC using sliding window correlation, it is essential that the duration of scan of all subjects are equal. It is also preferable if the scan parameters such as repetition time between each frame acquisition (TR) is identical for all of the subjects. Since ABIDE consists of data from various imaging sites, we do not have a single uniform TR for the entire dataset, rather we work with different scan parameter settings. The most common TR among the sites present in ABIDE is 2 s while a few of them have a different TR value. To handle this situation, we use linear interpolation on data from sites that have TR values other than 2 s and bring all of the data to a uniform TR setting (TR = 2 s).

For every subject, frames corresponding to the first 308 s (approximately 5 min) were selected and adjusted to 2 s TR, if required. This resulted in 154 frames (154 frames * 2 s TR = 308 s) for each subject. A sliding window of size 22 frames was slid in steps of 1 frame, resulting in 132 windowed correlations. Since these resultant correlation matrices are symmetric, only the upper triangular values of each matrix are extracted. The principal diagonal is also dropped since it contains self-correlation information of each brain region. The remaining features are then vectorized and used in subsequent steps.

Learning brain connectivity dynamics using clustering approach was practised in previously published studies [1, 25] and was observed to yield adequate characterization. However, a limitation to this approach is that the number of dynamic FC states (number of clusters, k value) has to be specified manually or determined using a criterion such as the elbow method. Research has revealed that brain dynamics matures with age, and is also influenced by the demographics of subjects being studied [19, 23]. The number of brain states revealed for adult subjects were higher in comparison to children [23], suggesting that a single k value may not be able to sufficiently characterize a highly diverse dataset such as the ABIDE dataset. Therefore, we implemented group clustering for k values ranging from 6 to 31 on all of the participant data to generate temporal properties and let the classifier learn the optimal features. Subject-wise mean lifetimes for each state is computed for all k values and stacked horizontally to generate a vector of size 481 for every subject. Finally, the classifier is trained on the dynamic temporal properties generated in the previous step (Fig. 1).

3.2 Classifier Methods

Machine learning classification methods, namely Support Vector Machines (SVM) [26], Random Forests (RF) [9], Extreme Gradient Boosting (XGB) [5, 7] and Deep Neural Networks (DNN) [16] were trained on both dynamic and static

features. Hyper-parameters were tuned over a sufficiently large search space. The classifiers were first tuned using random search over a large search space and then followed by a grid search on a finer and smaller search space consisting of high performing parameters.

4 Results and Discussion

Significant improvement in classification performance has been observed when dynamic features were used. The 10-fold cross-validation scores for all classifiers using both dynamic and static features are presented in Table 2. When dynamic features were used, all of the classifiers achieved accuracies greater than 71%, XGB being the highest performing classifier with 73.6% accuracy. In the case of static features, the classifiers demonstrated accuracies in the range of 65% to 70% and XGB outperformed the rest with an accuracy of 70.1%. It has to be noted that further optimization might increase performance of the classifiers, especially in the case of DNNs where the number of hyper-parameters are high and comprehensive optimization of the neural networks architecture is computationally expensive.

Table 2. Comparing classification performances of machine learning methods using Static FC and Dynamic FC features. (Classifier with the highest accuracy is boldfaced.)

Method	Accuracy	Sensitivity	Specificity	F1 score
SVM, Static	0.674	0.710	0.635	0.689
RF, Static	0.651	0.699	0.599	0.670
XGB, Static	0.701	0.719	0.682	0.710
DNN, Static	0.663	0.676	0.650	0.676
SVM, Dynamic	0.735	0.764	0.704	0.748
RF, Dynamic	0.717	0.759	0.673	0.733
XGB, Dynamic	0.736	0.750	0.720	0.744
DNN, Dynamic	0.710	0.713	0.706	0.714

To ascertain that there is a significant increase in classification accuracy, we performed a paired sample t-test on the 10-fold cross-validation accuracies generated for both static and dynamic features. We have 10 scores per each group, i.e. 10 scores generated using static features and 10 scores generated using dynamic features, and this gives a degree of freedom of 9 ($df = n - 1$). The results of the paired t-test are tabulated in Table 3 and we observe that in every case, the p-value obtained is less than the significance level (0.05). This demonstrates that using dynamic features has yielded a considerable increase in the classification performance.

Table 3. Results of paired sample t-test on the 10-fold cross-validation accuracies of methods using Static FC and Dynamic FC features. (2^{nd} and 3^{rd} columns show the mean 10-fold cross-validation accuracies of the corresponding method.)

Method	Static features accuracy	Dynamic features accuracy	P-value	T-value
SVM	0.674	0.735	0.001	4.549
RF	0.651	0.717	0.035	2.465
XGB	0.701	0.736	0.036	2.448
DNN	0.663	0.710	0.007	3.391

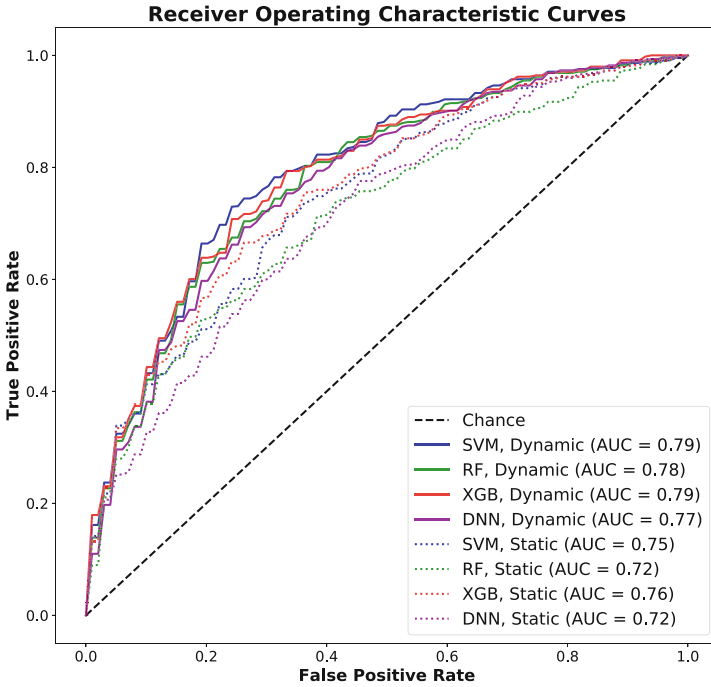


Fig. 2. ROC curves of methods using Static FC and Dynamic FC features.

Receiver operating characteristic (ROC) curves for all of the methods using both static and dynamic features are plotted in Fig. 2, along with their respective area under the curves (AUC). From the plot, we clearly notice that each method when using dynamic features outperforms its counterpart using static features. The AUCs ranged from 0.77 to 0.79 when dynamic features were used as opposed to 0.72 to 0.76 when static features were used.

The ability to harness the temporal properties of FC and use them in classification is what sets our approach apart from the previously reported ones. Most of the approaches relied on stationary FC for classification [8, 14, 21]. A classification method which took dynamic FC into consideration was published earlier

in the literature but the experiments presented in the paper were conducted on a relatively small dataset with 60 subjects (30 ASD, 30 TD) [22]. Our method has shown to be capable of handling large datasets while being relatively less expensive computationally.

The previously reported state-of-the-art accuracy was 70% [8] and the study was conducted on data from 17 different imaging sites with 1035 subjects (505 ASD, 530 TD). It has to be noted that fewer site-wise variations may lead to an increase in classification performance, and the accuracy drops as the population size increases [2, 8, 20]. Another recent study reported state-of-the-art accuracy of 71.4% using the AAL parcellation on a sample size of 774 subjects (379 ASD, 395 TD) [14].

Evidently, our approach has improved the state-of-the-art results by achieving an accuracy of 73.6% on a sample of 869 participants (423 ASD, 446 TD). However, as it has been discussed earlier that the site-wise variations and sample demographics have an impact on the performance of the model, caution should be taken while comparing studies conducted on different samples.

5 Conclusion

In this paper, we proposed a new framework that leverages brain dynamics for classifying autistic individuals and neurotypicals. Our work has shown that considering the dynamic nature of brain connectivity can yield improved results in the identification of autism. Usage of more advanced techniques for modeling the brain dynamics could further improve the diagnostic process.

References

1. Allen, E.A., Damaraju, E., Plis, S.M., Erhardt, E.B., Eichele, T., Calhoun, V.D.: Tracking whole-brain connectivity dynamics in the resting state. *Cereb. Cortex* **24**(3), 663–676 (2014)
2. Arbabshirani, M.R., Plis, S., Sui, J., Calhoun, V.D.: Single subject prediction of brain disorders in neuroimaging: promises and pitfalls. *Neuroimage* **145**, 137–165 (2017)
3. Aylward, E.H., et al.: MRI volumes of amygdala and hippocampus in non-mentally retarded autistic adolescents and adults. *Neurology* **53**(9), 2145–2145 (1999)
4. Chang, C., Glover, G.H.: Time-frequency dynamics of resting-state brain connectivity measured with fMRI. *Neuroimage* **50**(1), 81–98 (2010)
5. Chen, T., Guestrin, C.: XGBoost: a scalable tree boosting system. In: *Proceedings of the 22nd ACM SIGKDD International Conference on Knowledge Discovery and Data Mining*, pp. 785–794. ACM (2016)
6. Craddock, C., et al.: The neuro bureau preprocessing initiative: open sharing of preprocessed neuroimaging data and derivatives. *Neuroinformatics* (41) (2013)
7. Friedman, J.H.: Greedy function approximation: a gradient boosting machine. *Ann. Stat.* **29**(5), 1189–1232 (2001)
8. Heinsfeld, A.S., Franco, A.R., Craddock, R.C., Buchweitz, A., Meneguzzi, F.: Identification of autism spectrum disorder using deep learning and the ABIDE dataset. *NeuroImage Clin.* **17**, 16–23 (2018)

9. Ho, T.K.: Random decision forests. In: Proceedings of 3rd International Conference on Document Analysis and Recognition, vol. 1, pp. 278–282. IEEE (1995)
10. Huettel, S.A., Song, A.W., McCarthy, G., et al.: Functional magnetic resonance imaging, vol. 1. Sinauer Associates, Sunderland (2004)
11. Hutchison, R.M., et al.: Dynamic functional connectivity: promise, issues, and interpretations. *Neuroimage* **80**, 360–378 (2013)
12. Just, M.A., Keller, T.A., Kana, R.K.: A theory of autism based on frontal-posterior underconnectivity. In: *Development and Brain Systems in Autism*, pp. 35–63 (2013)
13. Kana, R.K., Keller, T.A., Cherkassky, V.L., Minshew, N.J., Just, M.A.: Atypical frontal-posterior synchronization of Theory of Mind regions in autism during mental state attribution. *Soc. Neurosci.* **4**(2), 135–152 (2009)
14. Khosla, M., Jamison, K., Kuceyeski, A., Sabuncu, M.R.: 3D convolutional neural networks for classification of functional connectomes. In: Stoyanov, D., et al. (eds.) *DLMIA/ML-CDS -2018. LNCS*, vol. 11045, pp. 137–145. Springer, Cham (2018). https://doi.org/10.1007/978-3-030-00889-5_16
15. Koshino, H., Carpenter, P.A., Minshew, N.J., Cherkassky, V.L., Keller, T.A., Just, M.A.: Functional connectivity in an fmri working memory task in high-functioning autism. *Neuroimage* **24**(3), 810–821 (2005)
16. LeCun, Y., Bengio, Y., Hinton, G.: Deep learning. *Nature* **521**(7553), 436 (2015)
17. Lord, C., Rutter, M., DiLavore, P.C., Risi, S., Gotham, K., Bishop, S., et al.: Autism diagnostic observation schedule: ADOS. Western Psychological Services, Los Angeles, CA (2012)
18. Ma, S., Calhoun, V.D., Phlypo, R., Adah, T.: Dynamic changes of spatial functional network connectivity in healthy individuals and schizophrenia patients using independent vector analysis. *NeuroImage* **90**, 196–206 (2014)
19. Naik, S., Subbareddy, O., Banerjee, A., Roy, D., Bapi, R.S.: Metastability of cortical bold signals in maturation and senescence. In: 2017 International Joint Conference on Neural Networks (IJCNN), pp. 4564–4570. IEEE (2017)
20. Nielsen, J.A., et al.: Multisite functional connectivity mri classification of autism: ABIDE results. *Front. Hum. Neurosci.* **7**, 599 (2013)
21. Plitt, M., Barnes, K.A., Martin, A.: Functional connectivity classification of autism identifies highly predictive brain features but falls short of biomarker standards. *NeuroImage Clin.* **7**, 359–366 (2015)
22. Price, T., Wee, C.-Y., Gao, W., Shen, D.: Multiple-network classification of childhood autism using functional connectivity dynamics. In: Golland, P., Hata, N., Barillot, C., Hornegger, J., Howe, R. (eds.) *MICCAI 2014. LNCS*, vol. 8675, pp. 177–184. Springer, Cham (2014). https://doi.org/10.1007/978-3-319-10443-0_23
23. Ryali, S., et al.: Temporal dynamics and developmental maturation of salience, default and central-executive network interactions revealed by variational bayes hidden Markov modeling. *PLoS Comput. Biol.* **12**(12), e1005138 (2016)
24. Schipul, S.E., Williams, D.L., Keller, T.A., Minshew, N.J., Just, M.A.: Distinctive neural processes during learning in autism. *Cereb. Cortex* **22**(4), 937–950 (2011)
25. Surampudi, S.G., Misra, J., Deco, G., Bapi, R.S., Sharma, A., Roy, D.: Resting state dynamics meets anatomical structure: temporal multiple kernel learning (tMKL) model. *NeuroImage* **184**, 609–620 (2019)
26. Vapnik, V.: The support vector method of function estimation. In: Suykens, J.A.K., Vandewalle, J. (eds.) *Nonlinear Modeling*, pp. 55–85. Springer, Boston (1998). https://doi.org/10.1007/978-1-4615-5703-6_3